International Journal of Innovative Research in Science, Engineering and Technology (IJIRSET)

| e-ISSN: 2319-8753, p-ISSN: 2320-6710| www.ijirset.com | Impact Factor: 7.512|

|| Volume 9, Issue 5, May 2020 ||

Comparative Analysis of Medical Image Segmentation with Extended Topological Active Net-based Optimizations

Pramila B[1], Dr. M B Meenavathi[2]

Associate Professor, Department of ECE, East West Institute of Technology, Bangalore, Karnataka, India[1]

Professor and Head, Department of EIE, Bangalore Institute of Technology, Bangalore, Karnataka, India[2]

ABSTRACT: Segmentation is an important image processing operation in computer aided diagnosis system. Tumors, cysts etc. must be segmented in medical images, before features are extracted from those regions for automated diagnosis. Accuracy of diagnosis is heavily dependent on segmentation precision. Towards this end, many segmentation algorithms have been proposed for medical image segmentation. In our earlier work [1] and [2], optimizations to extended topological active net (ETAN) has been proposed for higher accuracy in segmentation. This paper does a comparative analysis of the solution [1] and [2] with state of art methods for medical image segmentation. Medical images in different category of mammography, brain, ovary, retina and prostate gland are used for comparative analysis of segmentation and measuring the effectiveness of solutions proposed in [1] and [2].

KEYWORDS: TAN, ETAN, Deep learning and Objectiveness.

I. INTRODUCTION

Image segmentation operation partitions the image to multiple segments. It is a very important operation in automated computer aided diagnosis system and computer vision system. Once the image is partitioned to segments, features can be extracted from the interested segments. Machine learning classifiers are then trained with those features to classify tumors. In computer vision system segmentation is useful for various operations like object counting, object classification etc. The accuracy of applications are dependent heavily on how precisely the objects are segmented in the image. Many segmentation methods have been designed and ActiveNets is one such technique for image segmentation. It uses the concept of Deformable models (DM) [1]. In this method, a mesh is placed over the image and mesh surface is deformed in such way to fit the partitions of the image. The deformation process is guided by internal and external forces with goal of orientation of mesh towards objects of interest. Different types of ActiveNets are proposed by varying the deformation functions. Topological Active Net (TAN) and Extended Topological Active Net (ETAN) are two geometric deformable models applying energy-based functions to fit the 2D surface mesh over the image. The holes in the mesh are created to fit the objects of interest. Complex shapes like in case of medical images, cannot be segmented properly with ETAN. Also, there is a problem of hitting local minima. To solve these issues in earlier work [1] and [2], we have proposed optimizations to improve the performance of ETAN.

Work in [1] proposed a fuzzy rule-based optimization to improve the performance of ETAN. Work in [2] proposed Deep learning-based optimization to improve the performance of ETAN. In both the works, the solutions were not tested for medical images. In this work, a comparative analysis of both the optimizations against state of art segmentation methods is presented. The comparative analysis is done for medical images in different categories of brain, mammography, ovary, retina and prostate gland. The result of segmentation is compared against state of art methods to verify the effectiveness of the solution [1] and [2].

II. ETAN OPTIMIZATIONS

Two different machine learning optimizations are applied to improve the performance of ETAN

- Integrated Fuzzy rule-based optimization
- Deep Learning based optimization.

We adopted the following methodology for ETAN optimization.

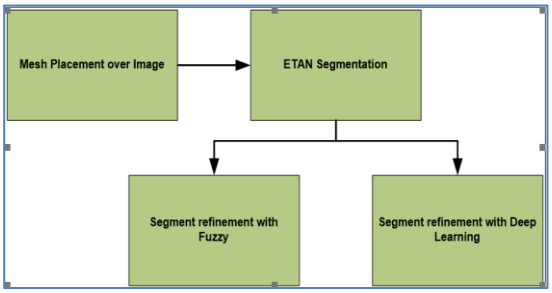

Fig. 1 Methodology for ETAN optimization

Rectangular mesh is placed over the image and ETAN segmentation is done on the image to split the image to segments. Each segment is then refined with Fuzzy optimization and Deep Learning optimization to refine the segments for the case of complex shapes.

III.INTEGRATED FUZZY OPTIMIZATION

The optimization applies two concepts of Objectiveness and Fuzzy learning-based rule base. The segmentation process in illustrated in the figure below

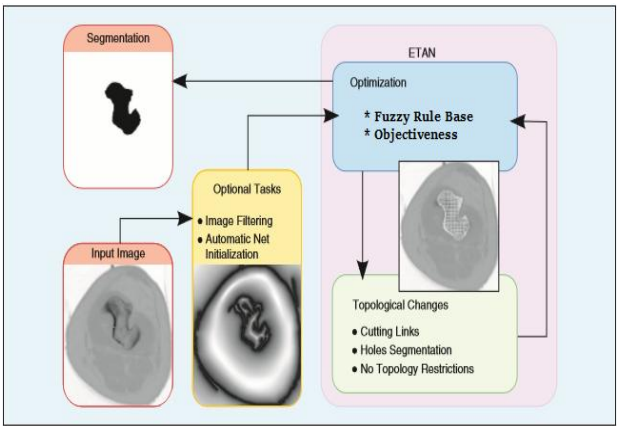

Fig. 2 Segmentation process

Objects in image are recognized using well defined closed boundaries and centers. Objectiveness is a measure of how likely an active mesh subnet is in foreground. The subnet lying on background should be removed. Different from previous approaches of deleting mesh links one by one, a subnet is removed as whole in this work speeding up the topology change due to holes creation and alignment to object surface.

Over the entire image mesh is placed and mesh is split to window of size nXn. For each window, a filter is applied to calculate the objectives score. Laplacian of a Gaussian filter of size 5X5 is applied. Areas of rapid changes in image(like edges) are detected with Laplacian filter. To reduce the noise sensitivity, image smoothing is done by applying Gaussian filter before Laplacian. This two-step process is referred as Laplacian of Gaussian (LoG).

$$L(x,y) = \nabla^2 f(x,y) = \frac{\partial^2 f(x,y)}{\partial x^2} + \frac{\partial^2 f(x,y)}{\partial y^2} \quad \text{Eqn 1}$$

To include smoothing, Gaussian and Laplacian is combined in one equation as

$$LoG(x,y) = -\frac{1}{\Pi\sigma^2}(1 - \frac{x^2+y^2}{2\sigma^2})e^{\frac{x^2+y^2}{2\sigma^2}} \quad \text{Eqn 2}$$

For uniform image, LoG value will be 0. When change occurs, LoG gives as positive or negative response depending on darker side or lighter side.

The objectiveness score for pixel is calculated from the Gaussian window as

| e-ISSN: 2319-8753, p-ISSN: 2320-6710| www.ijirset.com | Impact Factor: 7.512|

|| Volume 9, Issue 5, May 2020 ||

$PixObj(p) = \sum_{i=1}^{k} SiLoG(x,y)$ Eqn 3

Where Si is the objectiveness score of the windows containing pixel p and $LoG(x,y)$is the LOG value of the Gaussian window with x,y as the relative coordinate of the pixel p.

The Ob (Objectiveness) score for the whole of window region is calculated by summing the pixel wise objectiveness score. It is given as

$\mathrm{Ob(R)} = \sum_{i\varepsilon R} PixObj(p)$ Eqn 4

The $\mathrm{Ob(R)}$ value is thresholded (T) to decide if the region R is the part of foreground. If $\mathrm{Ob(R)}$ is below the threshold, then the mesh in that region is removed as background. The value of Threshold (T) is obtained by calculating Ob(R) for known set images split to patches and from the results, the best $\mathrm{Ob(R)}$ value which characterizes even a small object presence is decided as the threshold for isolation of background from foreground region.

IV. DEEP LEARNING OPTIMIZATION FOR ETAN

Deep learning-based optimization involves two steps of Convolutional neural network (CNN)based subnetting and ETAN based correction of subnet. Due to reduction in area of application of ETAN, the computation time is reduced and due to application of CNN the segmentation accuracy improves. The overall flow of the proposed solution is given below

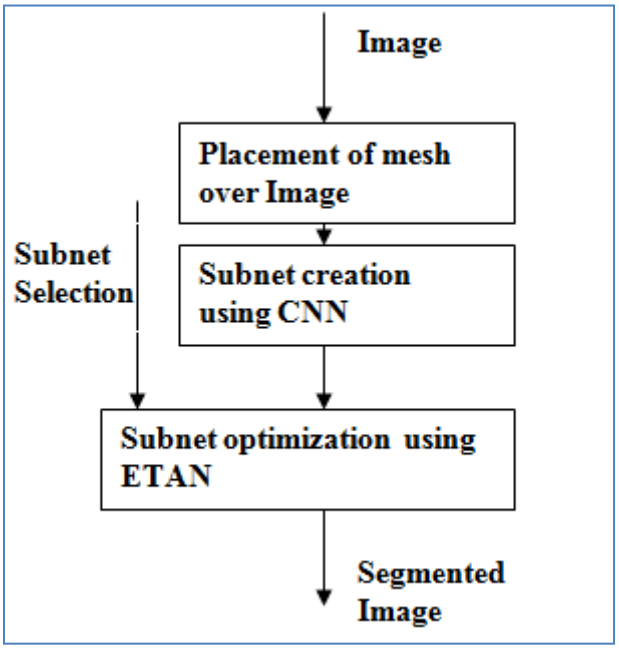

Fig. 3 Flow in Proposed Solution

A training dataset of images(marked with active net grids) of size N*X*N and its corresponding active subnet matrix as the class is prepared using BSDS500dataset. The subnet is represented is a binary matrix with 1 indicating the presence of link of the mesh and 0 indicating the absence of link. The goal is to train a CNN network that learns the features from the input to produce the active subnet matrix close to the ground truth.

Given an image to segment, the mesh is laid over whole image and passed to CNN based subnetting. The result from it is a mesh with holes for all background and mesh nodes are only on the objects. Some mesh nodes and links do cross the boundary, which must be detected and removed. This is achieved by ETAN energy minimization in each of the sub mesh. The overall process of optimization is given below

| e-ISSN: 2319-8753, p-ISSN: 2320-6710| www.ijirset.com | Impact Factor: 7.512|

|| Volume 9, Issue 5, May 2020 ||

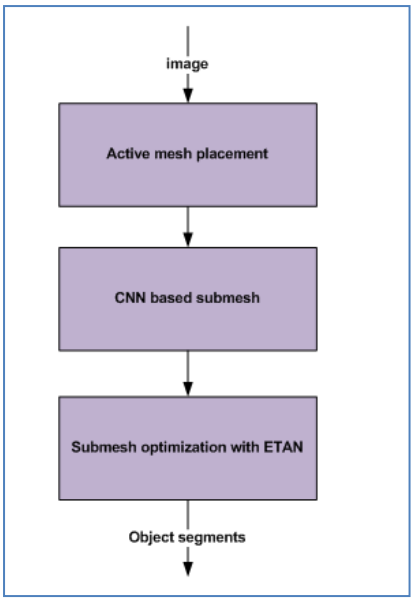

Fig. 4 Overall Process

V. COMPARATIVE ANALYSIS

The proposed solution was tested against medical images in following categories of

1. Brain
2. Mammography
3. Retina
4. Ovary
5. Prostate gland

The performance of proposed solutions [1] and [2] is compared against following state of art solutions

1. K-Mean clustering
2. Adaptive thresholding
3. Seed based Region growing segmentation
4. Watershed segmentation
5. Fuzzy C Mean Clustering

The performance of segmentation is compared in terms of following parameters

1. Accuracy
2. Sensitivity
3. Precision
4. RMSE
5. MAE

Accuracy(A) is calculated as

$$A = \frac{TP+TN}{TP+TN+FP+FN} \times 100 \quad \text{Eqn 5}$$

Sensitivity(S) is calculated as

$$S = \frac{TP}{TP+FN} \times 100 \quad \text{Eqn 6}$$

Precision (P) is calculated as

$$P = \frac{TP}{TP+FP} \times 100 \quad \text{Eqn 7}$$

20 Complex medical images in each of the five categories are used for testing. The images are split to small grids and each grid in the object of interest is marked. The segmented image is also split to grids and compared to marked grids

to decide the TP, TN, FP, FN. RMSE and MSE are calculated in comparison of grids falling in segmented result with grid marked.
The result for accuracy comparison is below:

Table 1 Accuracy comparison

Method	Accuracy
Integrated Fuzzy ETAN [1]	97.86
Deep learning ETAN [2]	96.54
K-Mean Clustering	84.5
Adaptive thresholding	86.2
Seed based region growing segmentation	87
Watershed segmentation	87.53
Fuzzy C mean clustering	88.15

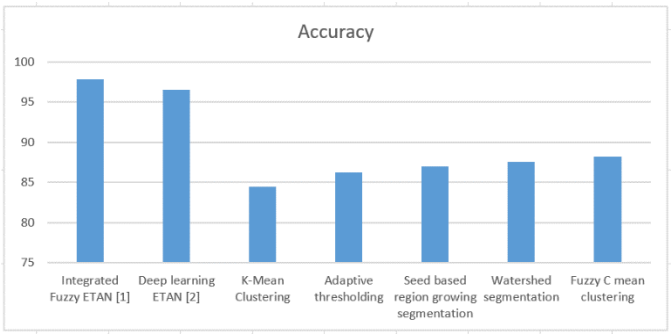

Fig. 5 Accuracy

The accuracy in integrated fuzzy ETAN and Deep learning ETAN is higher than state of art methods by great margin.
The result for sensitivity is below

Table 2 Sensitivity comparison

Method	Sensitivity
Integrated Fuzzy ETAN [1]	98.16
Deep learning ETAN [2]	97.14
K-Mean Clustering	85.5
Adaptive thresholding	87.12
Seed based region growing segmentation	88.14
Watershed segmentation	89.13
Fuzzy C mean clustering	89.87

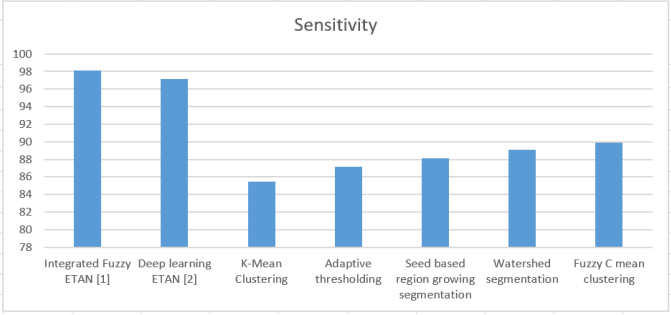

Fig. 6 Sensitivity comparison

The sensitivity in integrated fuzzy ETAN and Deep learning ETAN is higher than state of art methods.
The result for precision is below

Table 3 Precision comparison

Method	Precision
Integrated Fuzzy ETAN [1]	98.56
Deep learning ETAN [2]	97.34
K-Mean Clustering	84.45
Adaptive thresholding	86.12
Seed based region growing segmentation	87.34
Watershed segmentation	86.43
Fuzzy C mean clustering	88.97

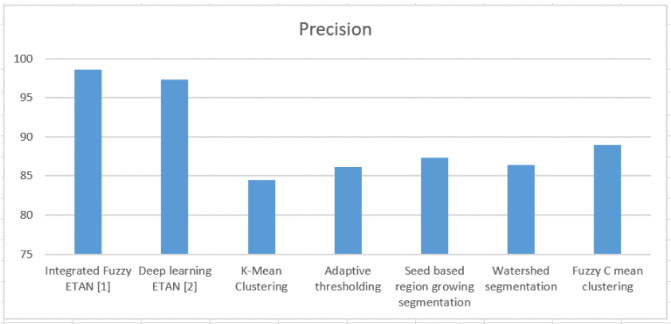

Fig. 7 Precision comparison

Precision is higher in the proposed solutions [1] and [2] than state of art segmentation methods.

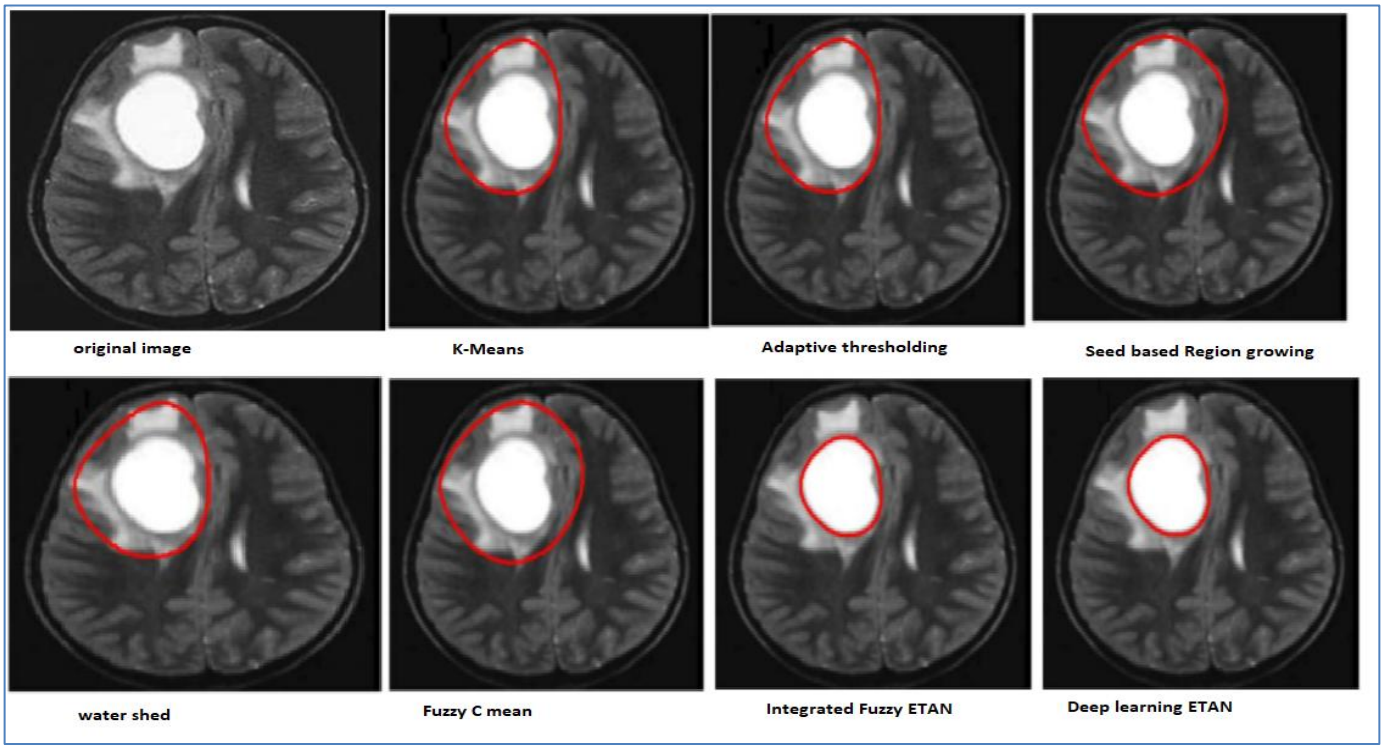

Fig. 8 Segmentation results

The result for RMSE is given below

Table 4 RMSE Comparison

Method	RMSE
Integrated Fuzzy ETAN [1]	0.0599
Deep learning ETAN [2]	0.0494
K-Mean Clustering	0.1413
Adaptive thresholding	0.1312
Seed based region growing segmentation	0.1311
Watershed segmentation	0.1211
Fuzzy C mean clustering	0.1156

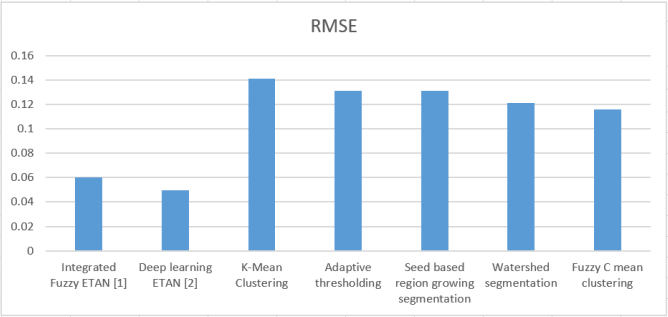

Fig. 9 RMSE

RMSE is lower in the proposed solution [1] and [2] compared to other state of art methods.
The result for MAE is given below

Table 5 MAE Comparison

Method	MAE
Integrated Fuzzy ETAN [1]	0.0011
Deep learning ETAN [2]	0.0010
K-Mean Clustering	0.0018
Adaptive thresholding	0.0019
Seed based region growing segmentation	0.0021
Watershed segmentation	0.0021
Fuzzy C mean clustering	0.0017

MAE is lower in the proposed solution [1] and [2] compared to other state of art methods.

VI. CONCLUSION

In this work, a comparative analysis of segmentation algorithms proposed in [1] and [2] is done against state of art segmentation approaches. For complex shapes in medical images, the solution [1] and [2] were found to have higher accuracy and lowest RMSE and MSE. The proposed optimizations have yielded very good segments close to expected result compared to other solutions. The result proves the effectiveness of proposed solutions [1] and [2] for medical image segmentation.

| e-ISSN: 2319-8753, p-ISSN: 2320-6710| www.ijirset.com | Impact Factor: 7.512|

|| Volume 9, Issue 5, May 2020 ||

REFERENCES

[1] Pramila B, Dr. M.B. Meenavathi"Fuzzy and Objectiveness Integrated Optimization of Extended Topological Active Net for Multi Object Segmentation", IJRTE, Vol 8, no.1, May 2019

[2] Pramila B, Dr. M.B. Meenavathi, "Deep Learning based Optimization of Extended Topological Active Net for Multi Object Segmentation,"IJAIEM, Vol 9, no.1, Jan 2020

[3] O. Ibanez, J.Santos, and M. G. Penedo, "Genetic approaches for topological active nets optimization," Pattern Recognition., vol. 42, no. 5, pp. 907–917, 2009.

[4] J. Novo, J. Santos, "Topological active models optimization with differential evolution," Expert Syst. Appl., vol. 39, no. 15, pp. 12165–12176, 2012.

[5] J. Novo, M. Penedo, "Evolutionary multiobjective optimization of topological active nets," Pattern Recogniton., Lett., vol. 31, no. 13, pp. 1781–1794, 2010.

[6] N. Bova, O. Cordón, "Image segmentation using extended topological active nets optimized by scatter search," IEEE Comput. Intell. Mag., vol. 8, no. 1, pp. 16–32, Feb. 2013.

[7] Li, Yuan-Long ,Qing. ".Fast Micro-Differential Evolution for Topological Active Net Optimization" IEEE transactions on cybernetics. 46. 10.1109/TCYB.2015.2437282.

[8] Cristina V. Sierra, Jos´eSantos "Emergent Segmentation of Topological Active Nets by Means of Evolutionary Obtained Artificial Neural Networks" In Proceedings of the 5th International Conference on Agents and Artificial Intelligence (ICAART-2013).

[9] N. Barreira,M. J. Santos "Automatic Topological Active Net Division in a Genetic-Greedy Hybrid Approach": Pattern Recognition and Image Analysis 2007.

[10] Tohka, J.: "Global optimization of deformable surface meshes based on genetic algorithms." In: Proceedings ICIAP, pp. 459–464. IEEE Computer Society Press, Los Alamitos (2001).

[11] C. McIntosh, G. Hamarneh, "Medial-based deformable models in nonconvex shape-spaces for medical image segmentation", *IEEE Trans. Med. Imag*, vol. 31, no. 1, pp. 33-50, 2012.

[12] X. Bresson, J.-P. Thiran, and S. Osher, "Fast global minimization of the active contour/snake model," J. Math. Imag. Vis., vol. 28, no. 2, pp. 151–167, Jun. 2007.

[13] GuoqiLiu , Haifeng Li, "Robust Evolution Method of Active Contour Models and Application in Segmentation of Image Sequence," Journal of Electrical and Computer Engineering, vol. 2018, 11 pages, 2018.

[14] Juan C. Moreno,V. B. S. Prasath "Brain MRI Segmentation with Fast and Globally Convex Multiphase Active Contours" arXiv,28 Aug 2013.

[15] GuodongWang ,Jie Xu, "Active Contour Model Coupling with Higher Order Diffusion for Medical Image Segmentation",Int J Biomed Imaging. 2014.

[16] Radhakrishna Achanta, Francisco Estrada, and Sabine S¨usstrunk, "Frequency-tuned salient region detection," 2009, pp. 1597–1604.

[17] Qiong Yan, Li Xu, "Hierarchical saliency detection," in IEEE Conference on Computer Vision and Pattern Recognition, 2013, pp. 1155–1162

[18] J.-J.HwangandT.-L.Liu. Pixel-wisedeeplearningforcontour detection. In ICLR, 2015

[19] K. Simonyan and A. Zisserman. Very deep convolutional networks for large-scale image recognition. In ICLR, 2015